Applied Environmental Research

Journal homepage : http://www.tci-thaijo.org/index.php/aer

Kaolin Modified Nano Zero Valent Iron Synthesis via Box-Behnken Design Optimization

Pummarin Khamdahsag[1], Wannakan Thongkao[2], Apichart Saowapakpongchai[2], Visanu Tanboonchuy[3,4,*]

[1] Environmental Research Institute, Chulalongkorn University, Bangkok, 10330, Thailand
[2] Department of Chemical Engineering, Faculty of Engineering, Thammasat University, Pathumthani, 12121, Thailand
[3] Department of Environmental Engineering, Faculty of Engineering,
[4] Research Center for Environmental and Hazardous Substance Management (EHSM), Khon Kaen University, Khon Kaen, 40002, Thailand
[*] Corresponding author: Email: visanu@kku.ac.th; Phone: +66 43202572 ext.113

Article History
Submitted: 23 December 2016/ Accepted: 24 April 2017/ Published online: 30 June 2017

Abstract

Nano zero valent iron (NZVI) has been extensively studied for its application to treat pollutants, particularly in contaminated water. This research studies enhancement of the reducing power of NZVI using kaolin as a supporter and ethanol as a medium. Kaolin modified nano zero valent iron (K-NZVI) was synthesized under three different parameters including ethanol content (0-100 v%), ratio of kaolin to NZVI (0-1.5), and dropping rate of $NaBH_4$ (4-10 mL/min). The Box-Behnken Design was used to design the experimental conditions, and Reactive Red 120 was used as an organic pollutant probe to quantify the reducing power of the synthesized K-NZVI. The results revealed that the highest reduction potential of K-NZVI was found under the following conditions: ethanol content of 100 v%, kaolin to NZVI ratio of 0.75, and $NaBH_4$ dropping rate of 7 mL/min. Based on these optimal synthesized conditions, the smaller crystal size of NZVI as measured from X-ray diffraction peaks, led to more efficient reduction of RR120. Images from scanning electron microscopy revealed that Fe was distributed uniformly over the surface, while the particles found in synthesized K-NZVI were mainly iron (Fe) and oxygen (O).

Keywords: Nano zero valent iron; Kaolin; Reactive red 120; Box-Behnken design

Introduction

Nano zero valent iron (NZVI) has been widely used to treat polluted groundwater and is also effectively used as an absorbent for various pollutants [1-2]. There are two major mechanisms for aqueous contaminant removal by NZVI, including physicochemical adsorption and oxidation-reduction reaction [3]. Pollutants removed by NZVI include halogenated hydro-carbons such as PCE, TCE, anions (e.g. NO^{3-}, $Cr_2O_7^{3-}$), organic compounds, heavy metals, and arsenic [4-8]. Also, NZVI is used as a moderate reducing agent in reduction reactions for the removal of hazardous substances. In this reaction, NZVI reacts with dissolved oxygen, water, and oxidants such as nitrate and possible contaminants. The hazardous substances can be made to react with NZVI to transform the mobile substances into immobile and less harmful species. Due to the presence of NZVI, the pH value is increased while the oxidation-reduction potential is decreased. The consumption of oxygen results an anaerobic environment while the reduction of water leads to the production of hydroxide as the reaction shown in Eq. 1 [9].

There are many methods for NZVI synthesis such as chemical method [10], sono-chemical [11], and thermal decomposition [12]. Of these, the chemical method is normally preferred for NZVI synthesis due to its ease and simplicity. Moreover, there is no need for complicated instruments or equipment for synthesis. However, the synthesized NZVI is often aggregate, leading to suboptimal efficiency. Consequently, various immobilization technologies are being developed for NZVI stabilization, such as starch-stabilized NZVI [13], zeolite-supported NZVI [14], guar gum-stabilized NZVI [15], and bentonite/iron nanoparticles [16]. These techniques encourage disaggregation and improve dispersion as well as stabilization. Kaolin is a NZVI supporter that is commonly available as a clay mineral with structural and chemical stability. Kaolin is also inexpensive, offering cost savings for upscaled production of NZVI. Above all, kaolin is effective not only as a supporter of NZVI, but is also itself an efficient adsorbent [17-22]. Kaolin is widely used as a porous material to adsorb pollutants from contaminated water and is thus an ideal support material for NZVI [23].

One drawback of the synthesized NZVI is that being easily oxidized to forms oxides and/or hydroxides iron such as Fe_3O_4, FeOOH, and Fe_2O_3 resulting in decrease of surface area with respect to active sites for reaction [24-26]. Therefore, using ethanol as medium during synthesis can prevent massive oxidation of synthesized NZVI [27].

Use of ethanol coupled with kaolin as a support material is not well researched in the literature. Thus, this research presents the method of kaolin modified nano zero valent iron (K-NZVI) synthesis using ethanol as medium. In order to evaluate the impact of parameters for synthesis, experiments were designed using the Box-Behnken Design (BBD), which is widely used in industry as an efficient research tool [28-29]. The findings of this work identified optimal conditions for synthesizing K-NZVI. Additionally, based on the BBD methodology, individual influences of parameters for synthesis on reducing capacity of the K-NZVI were observed as well via Reactive Red 120 (RR120) removal.

$$R\text{-}Cl + Fe^0 + H_2O \rightarrow R\text{-}H + Fe^{2+} + Cl^- + OH^- \quad \text{(Eq. 1)}$$

Experiment

1) K-NZVI synthesis.

The chemicals of reagent grade used in this study include $FeCl_3 \cdot 6H_2O$, $NaBH_4$, and 99.9% ethanol, (Merck). All chemical solutions were prepared using deionized water. $FeCl_3$ solution was provided by mixing 481.3 g of $FeCl_3 \cdot 6H_2O$ and kaolin in 100 mL of solution containing deionized water and ethanol. The amount of kaolin was calculated in order the gain weight ratio of kaolin to NZVI. This stage was considered as effecting the ethanol content and kaolin: NZVI ratio. $NaBH_4$ solution was prepared by dissolving 812.8 g of $NaBH_4$ with 40 mL of solution containing 30 v% of ethanol. After that, $NaBH_4$ was dropped into $FeCl_3$ solution under stirring, which was considered as the effect of dropping rate of $NABH_4$. The K-NZVI particles formed were separated from the liquid solution using a magnet. The three variables under investigation were (1) ethanol content; (2) kaolin to NZVI ratio; and (3) dropping rate of $NaBH_4$. The independent parameters and their range and levels are shown in Table 1. The results of a set of 15 experimental runs designed using a BBD are presented in Table 2.

Table 1 Range and level of independent parameters used for optimizing K-NZVI synthesized condition

Parameter	Representative	Range and level of actual value		
		-1	0	+1
Ethanol content (v%)	X_1	0	50	100
Kaolin : NZVI ratio	X_2	0	0.75	1.5
Dropping rate of $NaBH_4$ (mL/min)	X_3	4	7	10

Table 2 Various K-NZVI synthesized conditions in 15 experimental runs and percent removal of RR120 at 40 min from prediction and experiment

Run No.	Ethanol content (v%)	Kaolin : NZVI ratio	Dropping rate of $NaBH_4$ (mL/min)	% RR120 removal	
				Experiment	Predicted
1	50	1.5	4	84.1	84.6
2	50	0.75	7	86.6	86.8
3	0	0.75	4	81.4	80.7
4	0	0	7	70.7	72.5
5	50	0.75	7	85.9	86.8
6	50	0.75	7	87.9	86.8
7	100	0.75	4	99.1	100.5
8	0	1.5	7	76.6	76.8
9	50	0	10	74	73.6
10	100	1.5	7	96.5	94.7
11	50	0	4	73.5	72.4
12	100	0.75	10	91.2	91.9
13	100	0	7	95.9	95.7
14	50	1.5	10	63.5	64.7

15	0	0.75	10	72	70.6

2) Batch test

The synthesized K-NZVI obtained from each experimental run was tested immediately after synthesis using 100 ppm of RR120 (Ever Light Chemical Industry). The concentration of RR 120 was analyzed by using UV-VIS spectrometer at a maximum wavelength of 536 nm. After that, the RR120 removal efficiencies of the K-NZVI at 40 min of each experimental run were compared. The following formula was used to calculate the response value (percent RR120 removal) as shown in Eq. 2.

$$\text{RR120 removal (\%)} = 100 \times (C_0 - C_t)/C_0 \quad \text{(Eq. 2)}$$

where C_0 and C_t are initial and final concentrations of RR120 (ppm) after reaction time of 40 min with the K-NZVI, respectively.

3) K-NZVI characterization

Commercial NZVI (NANOFER STAR, NANO IRON s.r.o., Czech Republic) and the K-NZVI synthesized under conditions leading to the highest reducing power were characterized in regard to the presence of Fe^0 and crystalline size, using X-ray diffraction (XRD, Bruker D8 Advance) with a Cu Kα radiation source (λ = 1.5418 Å). The scan range of 2θ was 30-70° with increment and time step of 0.02° and 0.5 sec, respectively, to elucidate the matrix structures. Then, pH of zero point charge (pH_{pzc}) was measured following Mustafa's method [30]. Finally, morphology and chemical microanalysis was conducted using scanning electron microscopy (SEM, JEOL JSM-6400) coupled with energy dispersive X-ray spectroscopy (EDX). Specific surface area of the K-NZVI was also established by the Brunauer-Emmett-Teller (BET) method (Quantachrome instruments Autosorp-1).

Results and discussion

1) Reducing power test using BBD

The reducing power of K-NZVI under various synthesized conditions through degradation of RR120 at 40 min is shown in Table 1. Using BBD, the results were analyzed to check the normality of the residuals as shown in Figure 1. The data points on the normal probability plot presented in Figure 1(a) was reasonably close to a straight line, indicating no obvious problem with normality. Figure 1(b) presents the internal standardized residual plots versus fits value. The plot showed a random scatter, indicating constant variance of original observations for all response values. The histogram plot shown in Figure 1(c) reveals that the data also had no apparent problem with the normality of the curve. Figure 1(d) plots standardized residual versus batch runs of RR120 removal. The data points on this plot seemed to be a random pattern around the centre line, confirming that there was no abnormality in the observation order.

An empirical relationship followed by a second-order polynomial equation with interaction terms was fitted between the input parameters and the experimental results. An estimate function of RR120 removal efficiency was calculated and is presented in Eq.3, where Y is the prediction of RR120 removal (%), X_1 is ethanol content (v%), X_2 is kaolin to NZVI ratio, and X_3 is dropping rate of $NaBH_4$ (mL/min).

To consider the relationship between predicted and experimental values from the model calculated by Eq. 3, the data points obtained were very close to linear (R^2 = 0.9896), indicating that both values were accurate and reliable, as shown in Figure 2.

$$Y = 39.2653 + 0.0085X_1 + 37.9778X_2 + 9.42778X_3 + 0.002055X_1^2 - 12.4667X_2^2 - 0.66806X_3^2 - 0.0353333X_1X_2 + 0.0025X_1X_3 - 2.34444X_2X_3$$

or

Prediction of RR120 removal (%) = 39.2653 + 0.0085 ethanol content + 37.9778 kaolin to NZVI ratio + 9.42778 dropping rate of $NaBH_4$ + 0.002055 ethanol content^2 – 12.4667 kaolin to NZVI ratio^2 – 0.66806 dropping rate of $NaBH_4^2$ – 0.0353333 ethanol content · kaolin to NZVI ratio + 0.0025 ethanol content · dropping rate of $NaBH_4$ – 2.34444 kaolin to NZVI ratio · dropping rate of $NaBH_4$ (Eq. 3)

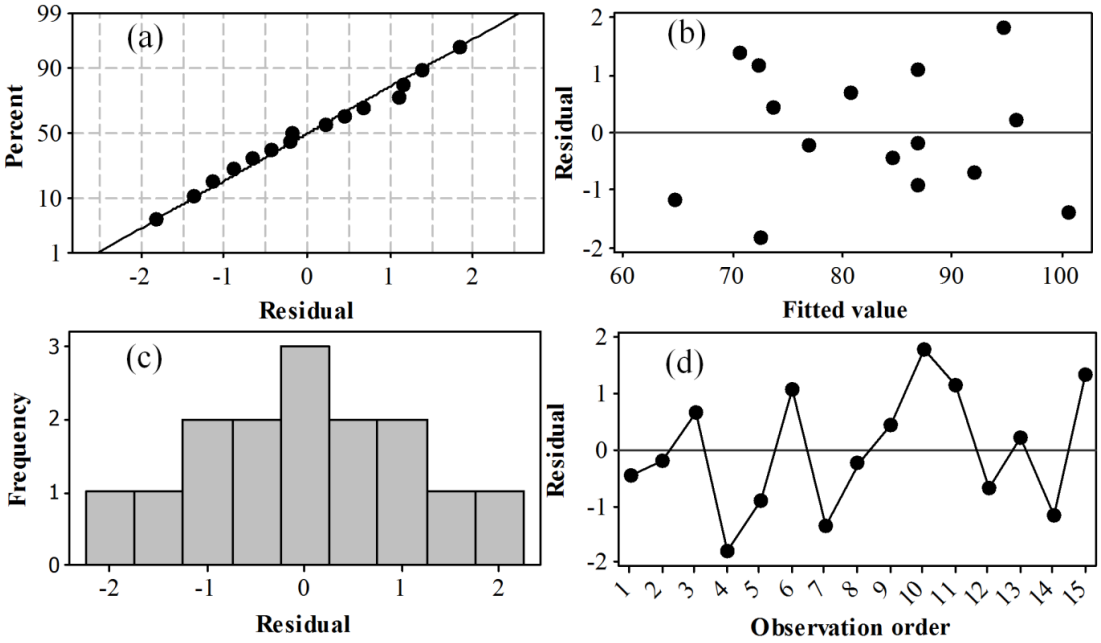

Figure 1 Internal standardized residual plots versus (a) normal probability, (b) fits, (c) histogram, and (d) observation order for percent removal of RR120 at 40 min.

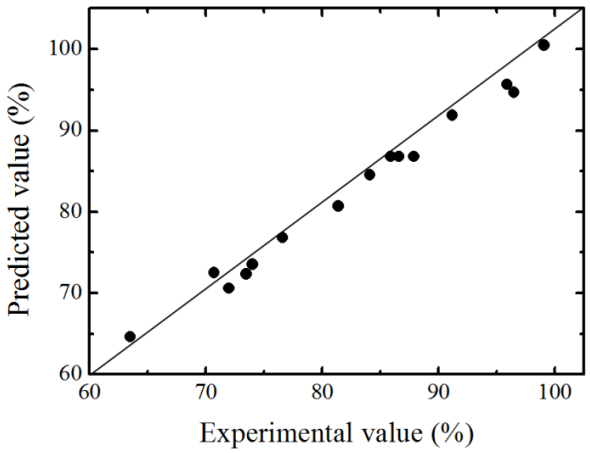

Figure 2 A parity plot of percent RR120 removal at 40 min (R^2 = 0.9896).

The optimum conditions were calculated by BBD. It was found that synthesis conditions of 100% of ethanol content, 0.75 kaolin to NZVI ratio, and 7 mL/min of $NaBH_4$ dropping rate gave the highest percent RR120 removal. To better understand the influences of the independent variables, contour and surface plots were employed. The results (shown in Figure 3) illustrate the relationship between percent removal of RR120 and the independent parameters. Figure 4 presents the main effects of the independent variables on RR120 removal,

which are represented in the contour and surface plots.

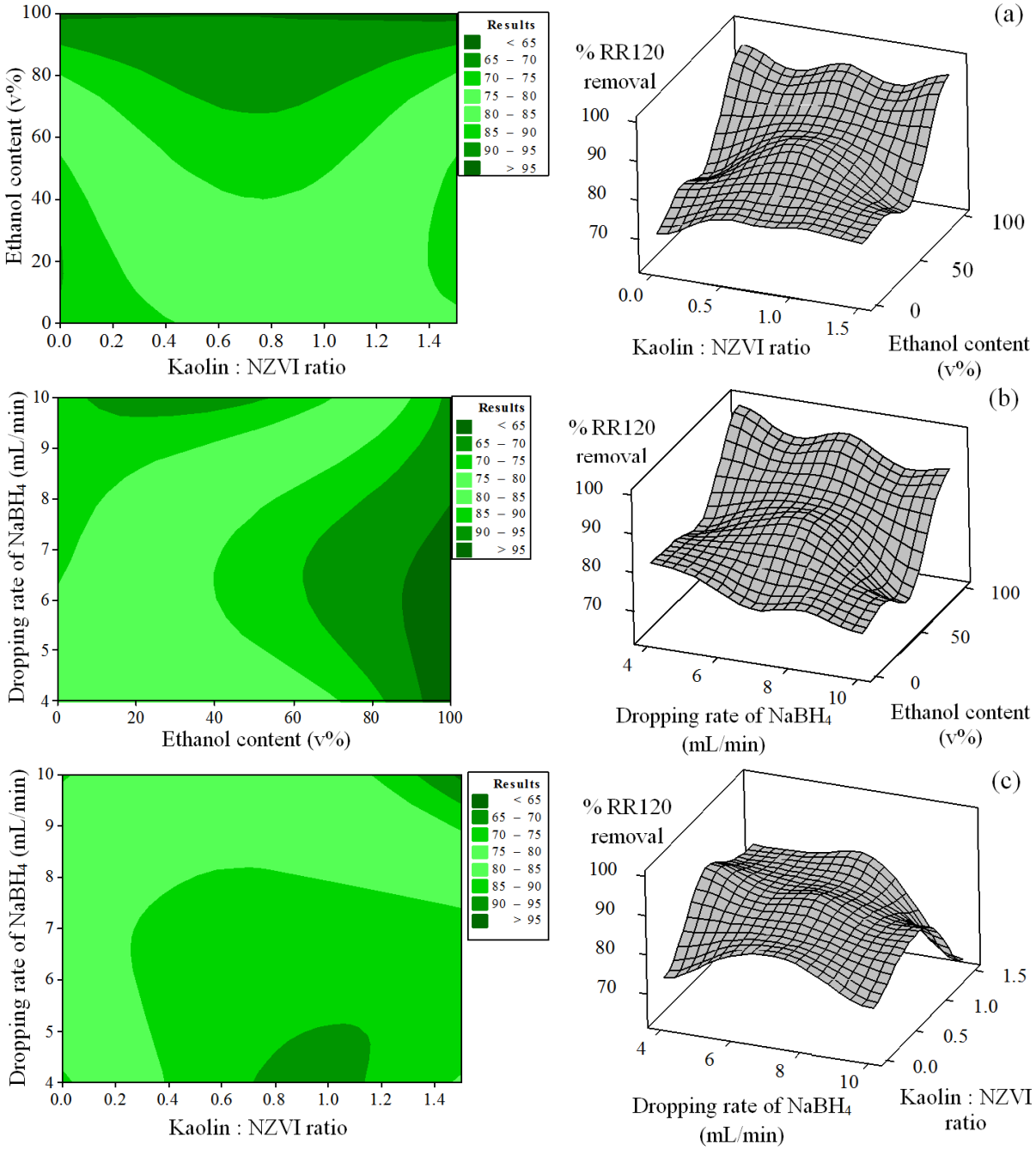

Figure 3 Contour and surface plots on effects of (a) ethanol content and kaolin: NZVI ratio, (b) ethanol content and dropping rate of $NaBH_4$, and (c) kaolin: NZVI ratio and dropping rate of $NaBH_4$.

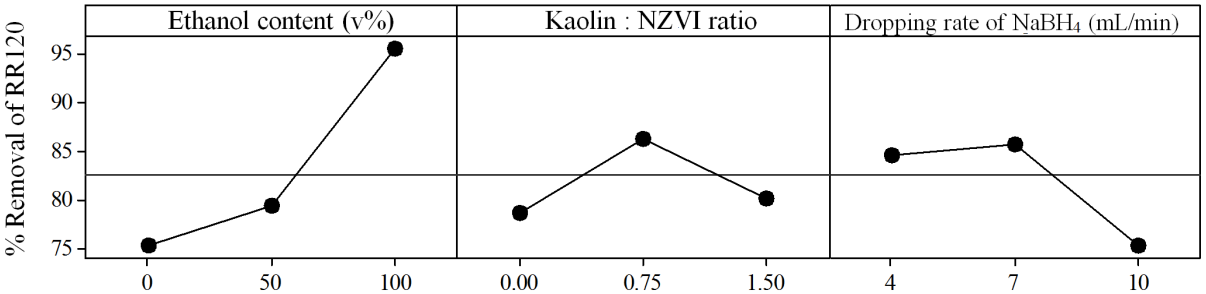

Figure 4 Main effect plots for percent removal of RR120 at 40 min.

Figure 4 reveals that increased ethanol concentration enhanced the reducing power of K-NZVI based on percent removal of RR120 because ethanol was capable of stabilizing nano-particles and preventing them from oxidation during NZVI synthesis. Having lower polarity than water, nanoparticles were more easily dispersed in the presence of ethanol. The higher the ethanol concentration, the higher the stability of the nanoparticles [27].

Kaolin has potential as a porous mineral to support and stabilize NZVI [31]. NZVI is modified by kaolin to form K-NZVI, which increases its mechanical strength resulting in better performance. However, the amount of kaolin added had no significant effect on K-NZVI performance. Moreover, for the effect of dropping rate of $NaBH_4$ (4, 7, and 10 mL/min), high reducing power was observed at slower dropping rates. The low dropping of $NaBH_4$ resulted in production of small particle size of NZVI, whereas rapid dropping caused aggregation of NZVI precipitates, reducing its surface area for reaction [32].

2) K-NZVI characterization

In Figure 5, the presence of NZVI (Fe0) was confirmed by XRD at 44.5°, plan (110), which was similar to the peak of the commercial NZVI. Due to high amount of iron in the commercial NZVI, the peak shifts to the left. Noise occurred in K-NZVI because of the presence of other compounds such as kaolinite and impurities [33]. However, iron oxides were also found from the XRD pattern of K-NZVI. Using the XRD software (Topas) crystalline sizes for synthesized K-NZVI and commercial NZVI were calculated at 51.3 nm and 88.3 nm, respectively. With an optimal kaolin : NZVI ratio of 0.75, kaolin as the modifier could reduce the crystalline size of NZVI, resulting in 99% efficiency in reducing RR120 after 40 minutes, compared with only 17.2% for commercial NZVI's.

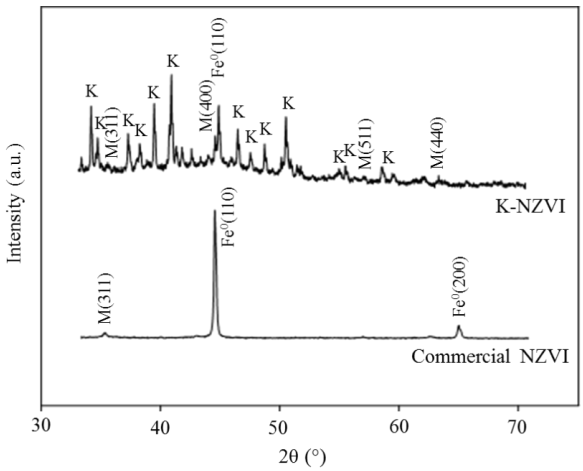

Figure 5 XRD patterns of K-NZVI and commercial NZVI, M=magnetite (Fe_3O_4) and/or maghemite (Fe_2O_3). K-NZVI synthesized conditions: 100% of ethanol content, 0.75 kaolin to NZVI weight ratio, and 7 mL/min of $NaBH_4$ dropping rate.

According to Figures 6 (a)-(d) and Table 3, the SEM image revealed that Fe was uniformly distributed across the surface, while the particles found in synthesized K-NZVI were mainly iron (Fe) and oxygen (O), corresponding to the XRD result. The iron oxides found in K-NZVI probably resulted from the drying process for the characterization study, when water molecules might lead to oxidation of iron [34]. Si and Al were barely found since the NZVI particles were adsorbed on the kaolin surface as revealed in the elemental mapping leading to reduce the Si and Al in EDX which mostly detected at the material's surface. Figure 6 (e) shows that the pH_{pzc} for the kaolin, lab-synthesized NZVI, and K-NZVI were around 9.5, 7.8, and 8.5, respectively. This implied that kaolin had an effect on the surface charge of K-NZVI, and also slightly increased its pH_{pzc}. RR120, an anionic reactive dye [35], is preferentially attracted to K-NZVI with a positive charge at pH<8.5, thus explaining the

higher efficiency of RR120 reduction. In this study, the RR120 initial pH 5.6-6.0 was found to provide optimal conditions for applying K-NZVI. After a 40 minute reaction time, the final solution pH increased to 8.0-10.0 due to the OH^- released from K-NZVI [36-37]; the K-NZVI removal efficiency would thereafter gradually be reduced. Additionally, surface area measured by BET method provided the results as follows: kaolin=12.03 m^2/g, NZVI= 9.98 m^2/g, and K-NZVI=8.45 m^2/g. The surface area of synthesized K-NZVI was the smallest as compared to NZVI and kaolin. This illustrates that replacement of NZVI results in a decrease in the surface area of the kaolin.

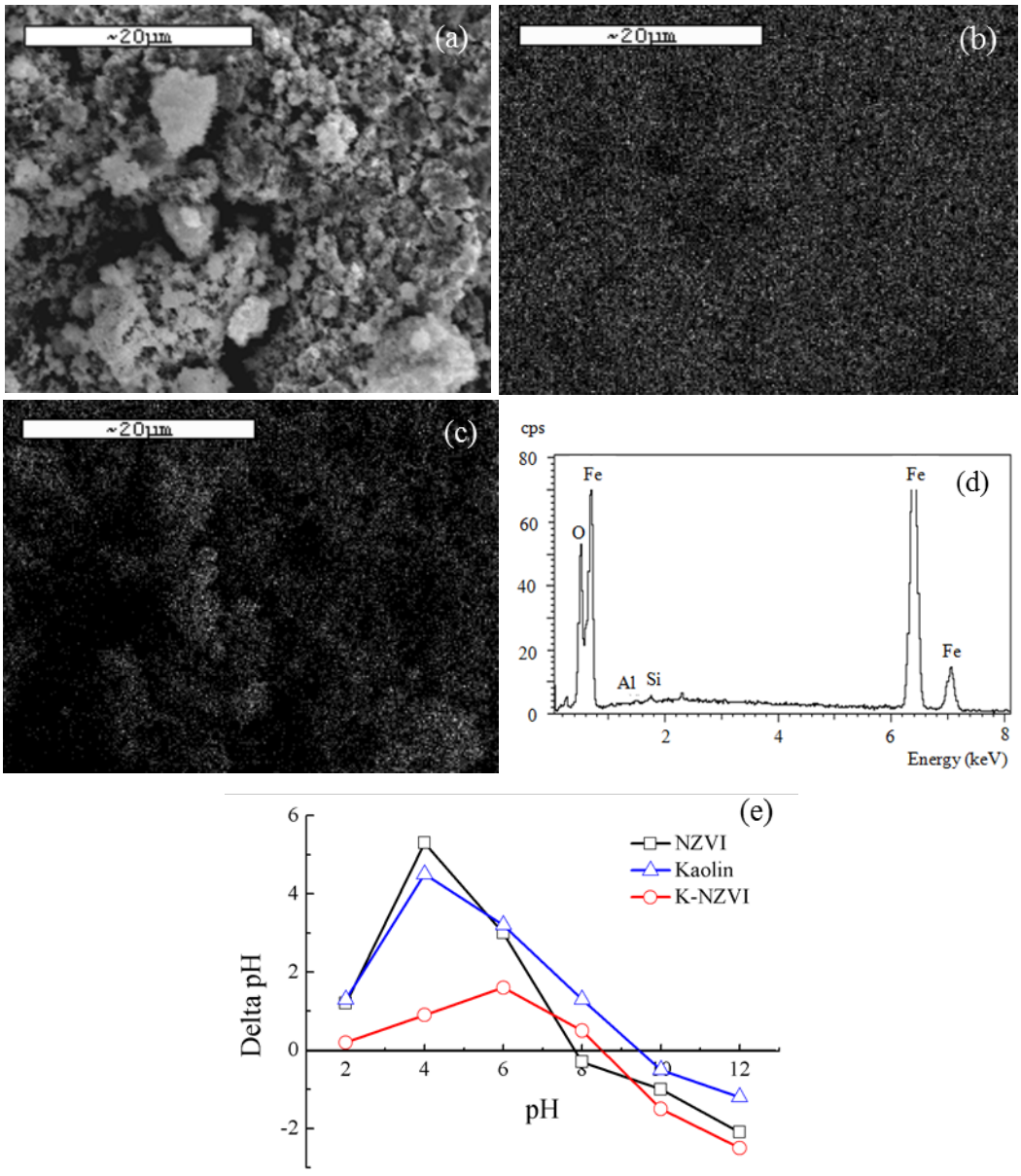

Figure 6 K-NZVI characterization: (a) SEM image, (b) elemental mapping of Fe, (c) elemental mapping of O, (d) SEM/EDX spectrum, and (e) pH_{pzc} plots. K-NZVI synthesized conditions: 100% of ethanol content, 0.75 kaolin to NZVI weight ratio, and 7 mL/min of $NaBH_4$ dropping rate.

Table 3 Element and atomic percentage ratio of K-NZVI analyzed by SEM/EDX. K-NZVI synthesized conditions: 100% of ethanol content, 0.75 kaolin to NZVI weight ratio, and 7 mL/min of $NaBH_4$ dropping rate

Element	Element %	Atomic %
O	25.95	54.69
Al	0.24	0.30
Si	0.42	0.50
S	0.44	0.46
Fe	72.95	44.04
Total	100.00	100.00

Conclusion

K-NZVI was optimally synthesized in this study using kaolin as a supporter and ethanol as a medium. BBD was applied as a design tool for determining optimal synthesis conditions of K-NZVI. In addition, RR120 was used as an organic pollutant probe to determine the reducing power of K-NZVI. Optimal synthesized conditions was found at 100 v% of ethanol content, 0.75 kaolin to NZVI ratio, and 7 mL/min of drip rate of $NaBH_4$. This indicated that the reducing power of K-NZVI increased under the synthesis conditions of high ethanol content and low drip rate of $NaBH_4$. In addition, the presence of kaolin enabled NZVI to improve its efficiency.

Acknowledgments

This research was supported by Research Center for Environmental and Hazardous Substance Management, Khon Kaen University, and National Research Council of Thailand.

References

[1] Bittern, M., Arditsoglou, A., Tsikouras, E., Voutsa, D. Arsenate removal by zero valent iron: batch and column tests. Journal of Hazardous Materials, 2007, 149, 548–552.

[2] Westerhoff, P., James, J. Nitrate removal in zero-valent iron packed columns. Water Research, 2003, 37, 1818-1830.

[3] Noubactep, C. Processes of contaminant removal in "Fe^0-H_2O" systems revisited: the importance of co-precipitation. The Open Environmental Engineering Journal, 2007, 1, 9-13.

[4] Wang, C.B., Zhang, W. Synthesizing nanoscale iron particles for rapid and complete dechlorination of TCE and PCBs. Environmental Science and Technology, 1997, 31, 2154-2156.

[5] Lien, H.L., Zhang, W. Transformation of chlorinated methanes by nanoscale iron particles. Journal of Environmental Engineering, 1999, 125, 1042-1047.

[6] Joo, S.H., Feitz, A.J., Sedlak, D.L., Waite, T.D. Quantification of the oxidizing capacity of nanoparticulate zerovalent iron. Environmental Science and Technology, 2005, 39, 1263-1268.

[7] Kanel, S.R., Greneche, J.M., Choi, H. Arsenic (V) removal from groundwater using nano scale zero-valent iron as a colloidal reactive barrier material. Environmental Science and Technology. 2006, 40, 2045-2050.

[8] Tanboonchuy, V., Grisdanurak, N., Liao, C.H. Background species effect on aqueous arsenic removal by nano zero-valent iron using fractional factorial design. Journal of Hazardous Materials. 2012, 205-206, 40-46.

[9] Mueller, N.C., Nowack, B. Nano zero-valent iron-The solution for water and soil remediation. Report of the Observatory NANO. 2010, 1-34.

[10] Glavee, G.N., Klabunde, K.J., Sorensen, C.M., Hadjipanayis, G.C. Chemistry of borohydride reduction of iron (II) and iron (III) ions in aqueous and nonaqueous

media. Formation of nanoscale Fe, FeB, and Fe_2B powders. Inorganic Chemistry. 1995, 34, 28-35.

[11] Khalil, H., Mahajan, D., Rafailovich, M., Gelfer, M., Pandya, K. Synthesis of zerovalent nanophase metal particles stabilized with poly (ethylene glycol). Langmuir. 2004, 20, 6896-6903.

[12] Amaraa, D., Felnerb, I., Nowikb, I., Margel, S. Synthesis and characterization of Fe and Fe_3O_4 nanoparticles by thermal decomposition of triiron dodecacarbonyl. Colloids and Surfaces A: Physicochemical and Engineering Aspects, 2009, 339, 106-110.

[13] He, F., Zhao, D.Y. Preparation and characterization of a new class of starch stabilized bimetallic nanoparticles for degradation of chlorinated hydrocarbons in water. Environmental Science and Technology, 2005, 39, 3314-3320.

[14] Li, Z.H., Jones, H.K., Zhang, P.F., Bowman, R.S. Chromate transport through columns packed with surfactant-modified zeolite/zero valent iron pellets. Chemosphere, 2007, 68, 1861-1866.

[15] Tiraferri, A., Chen, K.L., Sethi, R., Elimelech, M. Reduced aggregation and sedimentation of zero-valent iron nanoparticles in the presence of guar gum. Journal of Colloid and Interface Science, 2008, 324, 71-79.

[16] Shahwan, T., Üzüm, C., Eroglu, A.E., Lieberwirth, I. Synthesis and characterization of bentonite/iron nanoparticles and their application as adsorbent of cobaltions. Applied Clay Science, 2010, 47, 257-262.

[17] Obada, D.O., Dodoo-Arhin, D., Dauda, M., Anafi, F.O., Ahmed, A.S. and Ajayi, O.A. Potentials of fabricating porous ceramic bodies from kaolin for catalytic substrate applications. Applied Clay Science. 2016, 132-133, 194-204.

[18] Mohiuddin, E., Isa, Y.M., Mdleleni, M.M., Key, D. Effect of kaolin chemical reactivity on the formation of ZSM-5 and its physicochemical properties. Microporous and Mesoporous Materials. 2017, 237, 1-11.

[19] Lawal, I.A., Moodley, B. Column, kinetic and isotherm studies of PAH (phenanthrene) and dye (acid red) on kaolin modified with 1-hexyl, 3-decahexyl imidazolium ionic liquid. Journal of Environmental Chemical Engineering, 2016, 4, 2774-2784.

[20] Danková, Z., Bekényiová, A., Štyriaková, I., Fedorová, E. Study of Cu(II) adsorption by siderite and kaolin. Procedia Earth and Planetary Science, 2015, 15, 821-826.

[21] Rida, K., Bouraoui, S., Hadnine, S. Adsorption of methylenen blue from aqueous solution by kaolin and zeolite. Applied Clay Science, 2013, 83-84, 99-105.

[22] Yavuz, Ö., Saka, C. Surface modification with cold plasma application on kaolin and its effects on the adsorption of methylene blue. Applied Clay Science, 2013, 85, 96-102.

[23] Yuan, P., Annabi-Bergaya, F., Qao, Q., Fan, M.D., Liu, Z.W., Zhu, J.X., He, H.P., Chen, T.H. A combined study by XRD, FTIR, TG and HRTEM on the structure of delaminated Fe-intercalated/pillared clay. Journal of Colloid and Interface Science, 2008, 324, 142-149.

[24] Hwang, Y., Lee, Y.C., Mines, P.D., Huh, Y.S., Andersen, H.R. Nanoscale zero-valent iron (nZVI) synthesis in a Mg-aminoclay solution exhibits increased stability and reactivity for reductive decontamination. Applied Catalysis B: Environmental, 2014, 147, 748-755.

[25] Zhang, Y., Li, Y., Dai, C., Zhou, X., Zhang, W. Sequestration of Cd (II) with

nanoscale zero-valent iron (nZVI): Characterization and test in a two-stage system. Chemical Engineering Journal, 2014, 244, 218-226.

[26] Nakseedee, P., Tanboonchuy, V., Pimpha, N., Khemthong, P., Liao, C.H., Grisdanurak, N. Arsenic removal by nanoiron coupled with gas bubbling system. Journal of the Taiwan Institute of Chemical Engineers, 2015, 47, 182-189.

[27] Yuvakkumar, R., Elango, V., Rajendran, V., Kannan, N. Preparation and characterization of zero valent iron nanoparticles. Digest Journal of Nanomaterials and Biostructures, 2011, 6, 1771-1776.

[28] Berthouex, P.M., Brown, L.C. Statistics for Environmental Engineers. 2nd ed. Lewis Publishers, FL. 2002.

[29] Krasae, N., Wantala, K., Tantriratna, P., Grisdanurak, N. Removal of nitrate by bimetallic copper-nanoscale zero-valent iron (Cu-nZVI): Using 2k full factorial design. Applied Environmental Research, 2014, 36 (2), 15-23.

[30] Mustafa, S., Dilara, B., Nargis, K., Naeem, A., Shahida, P. Surface properties of the mixed oxides of iron and silica. Colloids and Surfaces A: Physicochemical and Engineering Aspects, 2002, 205, 273-282.

[31] Zhang, X., Shen, L., Zuliang, C., Mallavarapu, M., Ravendra, N. Kaolinite-Supported nanoscale zero-valent iron for removal of Pb^{2+} from aqueous solution: reactivity, characterisation and mechanism. Water Research. 2011, 45, 3481-3488.

[32] Choi, H.C., Giasuddin, A.B.M., Kanel, R. Method of synthesizing air-stable zero-valent iron nanoparticles at room temperature and applications. US Patent 2008/0091054, A1, 2008.

[33] González, J.A., Carreras, A.C., Kuiz, M. del C. Phase transformation in clays and kaolins produced by thermal treatment in chlorine and air atmosphere. Latin American Applied Research, 2007, 37(2), 133-139.

[34] Wang, Q., Snyder, S., Kim, J., Choi, H. Aqueous ethanol modified nanoscale zerovalent iron in bromate reduction: synthesis, characterization, and reactivity. Environmental Science and Technology, 2009, 43, 3292-3299.

[35] Senthilkumaar, S., Kalaamanib, P., Porkodia, K., Varadarajanc, P.R., Subburaamd, C.V. Adsorption of dis-solved Reactive red dye from aqueous phase onto activated carbon prepared from agricultural waste. Bioresource Technology, 2006, 97 (14), 1618-1625.

[36] Mishra, D., Farrell, J. Evaluation of mixed valent iron oxides as reactive adsorbents for arsenic removal. Environmental Science and Technology, 2005, 39, 9689-9694.

[37] Bang, S., Johnson, M.D., Korfiatis, G.P., Meng, X. Chemical reactions between arsenic and zero-valent iron in water. Water Research, 2005, 39, 763-770.